Flow Regime Map

❖ Co-current Flow in a Near-Horizontal Tube

✓ Intermittent flow: Mishima and Ishii (1980)

$$U_G - U_L = 0.487\sqrt{\frac{g(\rho_L - \rho_G)}{\rho_G}(D_H - h_L)} \quad (7.33)$$

– A larger $U_G - U_L$ value leads to the development of intermittent flow.

✓ For the transition from intermittent to bubbly flow

- Forces caused by turbulence >> buoyancy → **prevent coalescence**

$$U_L \geq \left[\frac{4A_G}{p_I}\frac{g\cos\theta}{f_L}\left(1 - \frac{\rho_G}{\rho_L}\right)\right]^{1/2}$$

Flow Regime Map

EXAMPLE 7.3. Water and air under atmospheric pressure and room temperature conditions flow co-currently in a long horizontal pipe that is 5 cm in diameter, under equilibrium conditions. The superficial velocities are $j_L = 0.1$ m/s and $j_G = 1.0$ m/s. Determine the two-phase flow regime in the pipe.

SOLUTION. The properties are similar to those calculated in Example 7.1. Since equilibrium conditions apply, we need to find the equilibrium stratified flow parameters first. The following equations are therefore solved simultaneously by trial and error: (7.22), (7.23), (7.24), (7.25) with f_I replaced with f_G, (7.26), and (7.27). Other equations are $j_L = U_L(1 - \alpha)$, $j_G = U_G\alpha$, $f_G = C_G \mathrm{Re}_G^{-m}$, $f_L = C_L \mathrm{Re}_L^{-m}$, and

$$\mathrm{Re}_G = \rho_G D_G U_G / \mu_G,$$

$$\mathrm{Re}_L = \rho_L D_L U_L / \mu_L,$$

$$D_G = \frac{2\pi - (\gamma - \sin\gamma)}{2\pi - \gamma + 2\sin(\gamma/2)} D,$$

$$D_L = \frac{\gamma - \sin\gamma}{\gamma + 2\sin(\gamma/2)} D,$$

$$p_L = \gamma D/2,$$

$$p_G = (2\pi - \gamma) D/2,$$

$$p_I = D\sin(\gamma/2)$$

Flow Regime Map

The iterative solution of these equations leads to

$$h_{\mathrm{L}} = 0.036\,\mathrm{m},$$
$$\alpha = 0.227,$$
$$U_{\mathrm{G}} = 4.14\,\mathrm{m/s},$$
$$U_{\mathrm{L}} = 0.129\,\mathrm{m/s}.$$

We can now examine the criterion of Mishima and Ishii, Eq. (7.33). The right-hand side of the latter equation is found to be 5.21 m/s, which is clearly larger than $U_{\mathrm{G}} - U_{\mathrm{L}}$. A regime transition out of stratified flow does not occur, and therefore the flow pattern is stratified.

The right-hand side of Eq. (7.28) is calculated to be 0.165 m/s. Since $U_{\mathrm{G}} > 0.165$ m/s, therefore the flow pattern is stratified wavy.

An alternative to Eq. (7.33) is Eq. (7.31). Instead of Eq. (7.31), however, we will use the criterion of Eq. (7.32), which is essentially a curve fit to the results of Eq. (7.31) for the critical conditions for horizontal flow. Thus,

$$x = \frac{\rho_{\mathrm{G}} j_{\mathrm{G}}}{\rho_{\mathrm{G}} j_{\mathrm{G}} + \rho_{\mathrm{L}} j_{\mathrm{L}}} = 0.0117, \qquad X_{\mathrm{tt}} = \left(\frac{1-x}{x}\right)^{0.9} \left(\frac{\mu_{\mathrm{L}}}{\mu_{\mathrm{G}}}\right)^{0.1} \left(\frac{\rho_{\mathrm{G}}}{\rho_{\mathrm{L}}}\right)^{0.5} = 2.745.$$

From Eq. (7.30), we get $\mathrm{Fr} = 0.0493$. The right-hand side of Eq. (7.32) is calculated to be 0.1388. We thus have the following condition, which implies that the flow regime is stratified:

$$\mathrm{Fr} < \left(\frac{1}{0.65 + 1.11 X_{\mathrm{tt}}^{0.6}}\right)^2.$$

Flow Regime Map

- Two-phase flow in an inclined tube (Barnea, Taitel, and co-workers)
  - ✓ Unified model for all pipe angles
  - ✓ Bubbly-slug
    - a stable bubbly flow becomes impossible if the rise velocity of Taylor bubbles is lower than the velocity of regular bubbles

$$0.35\sqrt{gD}\sin\theta + 0.54\sqrt{gD}\cos\theta < 1.53\left[\frac{\sigma g \Delta\rho}{\rho_L^2}\right]^{1/4}\sin\theta$$

$$0.35\sqrt{gD} \le 1.53[g\Delta\rho\sigma/\rho_L^2]^{1/4}$$ For vertical tube

  - ✓ Transition to the finely dispersed bubbly flow regime

$$d_B < d_{cb} \text{ and } d_B < d_{cr}$$

$$d_B = (0.725 + 4.15\alpha^{1/2})\left(\frac{\sigma}{\rho_L}\right)^{3/5}\varepsilon^{-2/5},\quad d_{cr} = 2\left[\frac{0.4\sigma}{\Delta\rho g}\right]^{1/2},\ d_{cb} = \frac{3}{8}\frac{\rho_L}{\Delta\rho}\frac{f_M j^2}{g\cos\theta}.$$

$$\varepsilon = -\left(\frac{dP}{dz}\right)_{fr} j = \frac{2f_M}{D}j^3 \qquad f_M = 0.046(jD/\nu_L)^{-0.2}$$

Flow Regime Map

- Two-phase flow in an inclined tube (Barnea, Taitel, and co-workers)
  - ✓ Disruption mechanism of annular flow regime
    - The formation of lumps of liquid (likely to happen when liquid film is very thick)
    - Film instability
  - ✓ Separated flow momentum equation

$$\frac{\tau_w p_f}{A} + \frac{\tau_I p_I}{A}\left(\frac{1}{1-\alpha} + \frac{1}{\alpha}\right) - \Delta\rho g \sin\theta = 0 \qquad A = \pi D/4, \quad p_f = \pi D, \quad p_I = \pi D\sqrt{\alpha}, \quad \alpha = 1 - \frac{2\delta_F}{D}$$

$$\tau_I = f_I \rho_G \frac{1}{2}\frac{j_L^2}{(1-\alpha)^2} \qquad f_I = f_G\left(1 + \frac{300\delta_F}{D}\right), \qquad \tau_w = f_w \frac{1}{2}\rho_L \frac{j_L^2}{(1-\alpha)^2}$$

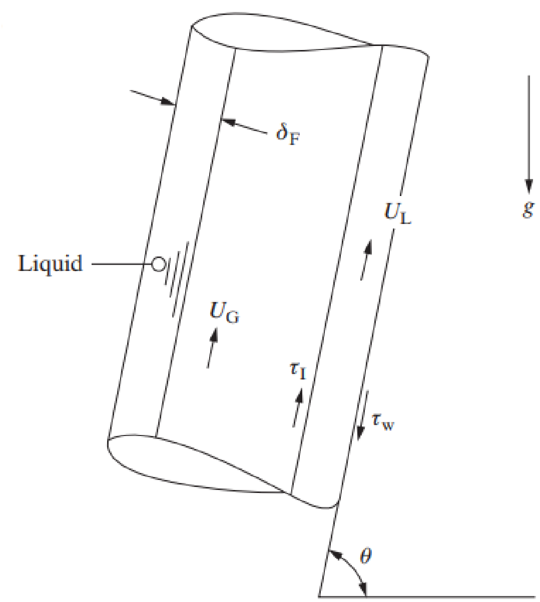

- f_g, f_w: single-phase models
- Then, α can be obtained.

Flow Regime Map

- Two-phase flow in an inclined tube (Barnea, Taitel, and co-workers)
  - ✓ Disruption mechanism of annular flow regime
    - Disruption of the annular flow regime for mechanism (a)

$$1 - \alpha > \frac{1}{2}(1-\alpha)_{\max},\ (1-\alpha)_{\max} = 0.48.$$

    - For mechanism (b),

$$\delta_{\mathrm{F}} \geq \delta_{\mathrm{F,\,crit}} \qquad \frac{\partial \tau_{\mathrm{I}}}{\partial \delta_{\mathrm{F}}} = 0. \quad \text{for } \delta_{F,crit} \qquad \alpha = 1 - \frac{2\delta_{\mathrm{F}}}{D}$$

IATE (dynamic flow regime model)

- History
  - ✓ Ishii (1975)
  - ✓ Revankar and Ishii, 1992; Kocamustafaogullari and Ishii, 1995; Millies et al., 1996; Morel et al., 1999; Wu et al., 1998; Kim et al., 2002; Hibiki and Ishii, 2001; Ishii et al., 2002; Sun et al., 2004a, b; Ishii and Hibiki, 2011
- Application to TH codes
  - ✓ VIPRE-02, thermal-hydraulics code
  - ✓ CULDESAC, a three-fluid model for vapor explosion analysis
- Still in development

IATE (dynamic flow regime model)

- Number density equation
  - ✓ Distribution function

$$f(V_\mathrm{P}, \vec{x}, \vec{U}_\mathrm{P}, t) = \text{distribution function of particles of the dispersed phase [in particles/m}^6\text{(m/s)}^3]$$

  - ✓ Total number of particles per unit mixture volume at time t and location $\vec{x}$

$$n_\mathrm{P}(\vec{x}, t) = \int_{V_{\mathrm{P,min}}}^{V_{\mathrm{P,max}}} \int_{U_{\mathrm{P},x,\mathrm{min}}}^{U_{\mathrm{P},x,\mathrm{max}}} \int_{U_{\mathrm{P},y,\mathrm{min}}}^{U_{\mathrm{P},y,\mathrm{max}}} \int_{U_{\mathrm{P},z,\mathrm{min}}}^{U_{\mathrm{P},z,\mathrm{max}}} f(V_\mathrm{P}, \vec{x}, \vec{U}_\mathrm{P}, t) dV_\mathrm{P} dU_{\mathrm{P},x} dU_{\mathrm{P},y} dU_{\mathrm{P},z}$$

  - ✓ Assumption for simplicity: $f = f(V_\mathrm{P}, \vec{x}, t)$

$$\frac{\partial f}{\partial t} + \nabla\cdot(f\vec{U}_\mathrm{P}) + \frac{\partial}{\partial V_\mathrm{P}}\left(f\frac{dV_\mathrm{P}}{dt}\right) = \sum_j S_j + S_\mathrm{ph}$$

Source and sink terms: collapse, breakup, coalescence

Source term from phase change

$\int_{V_{\mathrm{P,min}}}^{V_{\mathrm{P,max}}} dV_\mathrm{P}$

$$\frac{\partial n_\mathrm{P}}{\partial t} + \nabla.(n_\mathrm{P}\vec{U}_{\mathrm{P,m}}) = \sum R_j + R_\mathrm{ph}$$

$$\vec{U}_{\mathrm{P,m}} = \frac{1}{n_\mathrm{P}} \int_{V_{\mathrm{P,min}}}^{V_{\mathrm{P,max}}} f(V_\mathrm{P}, \vec{x}, t)\vec{U}_\mathrm{P}(V_\mathrm{P}, \vec{x}, t) dV_\mathrm{P}$$

IATE (dynamic flow regime model)

- Interfacial area transport equation

$$\frac{\partial f}{\partial t} + \nabla\cdot(f\vec{U}_{\mathrm{P}}) + \frac{\partial}{\partial V_{\mathrm{P}}}\left(f\frac{dV_{\mathrm{P}}}{dt}\right) = \sum_j S_j + S_{\mathrm{ph}} \qquad \frac{\partial n_{\mathrm{P}}}{\partial t} + \nabla.(n_{\mathrm{P}}\vec{U}_{\mathrm{P,m}}) = \sum R_j + R_{\mathrm{ph}}$$

✓ Multiplying the particle surface area, and integrating the product over the entire distribution function f

$$\frac{\partial a_{\mathrm{I}}''}{\partial t} + \nabla\cdot(a_{\mathrm{I}}''\vec{U}_{\mathrm{I}}) = \frac{2}{3}\left(\frac{a_{\mathrm{I}}''}{\alpha}\right)\left[\frac{\partial \alpha}{\partial t} + \nabla\cdot(\alpha\vec{U}_{\mathrm{G}}) - \dot{Q}_{\mathrm{ph}}\right] + \int_{V_{\mathrm{P,min}}}^{V_{\mathrm{P,max}}}\left(\sum_j S_j + S_{\mathrm{ph}}\right)A_{\mathrm{P}}dV_{\mathrm{P}}$$

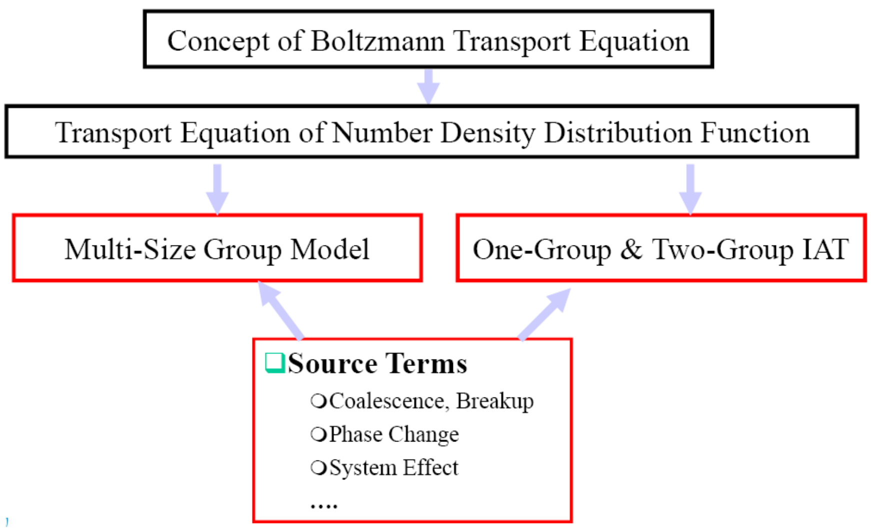

Q_{ph} : total volumetric gas generation rate from phase change per unit mixture volume

A_P: the average surface area of the fluid particles that have volume V_P

$$\vec{U}_{\mathrm{I}}(\vec{x},t) = \frac{\int_{V_{\mathrm{P,min}}}^{V_{\mathrm{P,max}}} f(V_{\mathrm{P}},\vec{x},t)A_{\mathrm{P}}(V_{\mathrm{P}})\vec{U}_{\mathrm{P}}(V_{\mathrm{P}},\vec{x},t)dV_{\mathrm{P}}}{\int_{V_{\mathrm{P,min}}}^{V_{\mathrm{P,max}}} (V_{\mathrm{P}},\vec{x},t)A_{\mathrm{P}}(V_{\mathrm{P}})dV_{\mathrm{P}}}$$

IATE (dynamic flow regime model)

- Simplification of Interfacial area transport equation
  - Major challenge: complexity of the source and sink terms
  - Bubbly flow for simplification

$$\int_{V_{\mathrm{P,min}}}^{V_{\mathrm{P,max}}} \sum_j S_j dV_{\mathrm{P}} = \sum_j R_j \qquad \int_{V_{\mathrm{P,min}}}^{V_{\mathrm{P,max}}} \sum_j S_j A_{\mathrm{P}} dV_{\mathrm{P}} = \sum_j R_j \Delta A_{\mathrm{P}}$$

  - Assumptions
    - The coalescence of two equal-volume bubbles leads to a single bubble
    - Breakup of a bubble leads to two-equal volume bubbles
    - The bubbles resulting from nucleation have a diameter of d_{Bc} at birth

$$n_{\mathrm{P}} = \psi \frac{(a_{\mathrm{I}}'')^3}{\alpha^2},$$

$$\psi = \frac{1}{36\pi}(d_{\mathrm{Sm}}/d_{\mathrm{C}})^3,$$

$$\Delta A_{\mathrm{P}} = \begin{cases} -0.413 A_{\mathrm{P}} & \text{for coalescence,} \\ 0.260 A_{\mathrm{P}} & \text{for breakup,} \end{cases}$$

$$d_{\mathrm{Sm}} = \frac{6\alpha}{a_{\mathrm{I}}''} \quad \text{(Sauter mean diameter),}$$

$$d_{\mathrm{C}} = \left(\frac{6V_{\mathrm{P}}}{\pi}\right)^{1/3} \text{(volume-equivalent diameter).}$$

IATE (dynamic flow regime model)

- Simplification of Interfacial area transport equation

$$\frac{\partial a_{\mathrm{I}}''}{\partial t} + \nabla\cdot(a_{\mathrm{I}}''\vec{U}_{\mathrm{I}}) = \frac{2}{3}\left(\frac{a_{\mathrm{I}}''}{\alpha}\right)\left[\frac{\partial \alpha}{\partial t} + \nabla\cdot(\alpha\vec{U}_{\mathrm{G}}) - \dot{Q}_{\mathrm{ph}}\right] + \int_{V_{\mathrm{P,min}}}^{V_{\mathrm{P,max}}}\left(\sum_j S_j + S_{\mathrm{ph}}\right)A_{\mathrm{P}}dV_{\mathrm{P}}$$

$$\frac{\partial a_{\mathrm{I}}''}{\partial t} + \nabla.(a_{\mathrm{I}}''\vec{U}_{\mathrm{I}}) = \frac{2}{3}\frac{a_{\mathrm{I}}''}{\alpha}\left[\frac{\partial \alpha}{\partial t} + \nabla.(\alpha\vec{U}_{\mathrm{G}}) - \dot{Q}_{\mathrm{Ph}}\right] + \frac{1}{3\psi}\left(\frac{\alpha}{a_{\mathrm{I}}''}\right)^2\sum_j R_j + \pi d_{\mathrm{Bc}}^2 R_{\mathrm{Ph}}$$

- One-group IATE
  - ✓ Spherical and uniform bubble size
  - ✓ Uniform nucleation bubble size
  - ✓ Nucleation-generated bubbles that are much smaller than regular bubbles
  - ✓ $d_{Sm} = d_C \quad \psi = 1/36\pi$
  - ✓ Area averaging

$$\langle \vec{U}_{\mathrm{I}} \rangle \equiv \frac{\langle \vec{U}_{\mathrm{I}} a_{\mathrm{I}}'' \rangle}{\langle a_{\mathrm{I}}'' \rangle} \approx \langle \vec{U}_{\mathrm{G}} \rangle_{\mathrm{G}}$$

IATE (dynamic flow regime model)

- Based on steady-state adiabatic air–water experiments in vertical channel
  - ✓ Break-up by turbulent eddies

$$R_{\mathrm{TI}} = C_{\mathrm{TI}} \left(\frac{n_{\mathrm{P}} u_t}{d_{\mathrm{P}}} \right) \exp\left(-\frac{\mathrm{We}_{\mathrm{cr}}}{\mathrm{We}} \right) \sqrt{1 - \frac{\mathrm{We}_{\mathrm{cr}}}{\mathrm{We}}}$$

$$C_{\mathrm{TI}} = 0.085,$$

$$\mathrm{We}_{\mathrm{cr}} = 6.0 \qquad \text{(critical Weber number)}$$

$$\mathrm{We} = \rho_{\mathrm{L}} d_{\mathrm{P}} u_{\mathrm{t}}^2 / \sigma \qquad \text{(bubble Weber number).}$$

- u_t: the root mean square of turbulent velocity fluctuations

$$u_{\mathrm{t}} = \sqrt{\overline{\Delta u'^2}} \approx 1.38 \varepsilon^{1/3} d_{\mathrm{P}}^{1/3}$$

  - ✓ Collision-induced coalescence

$$R_{\mathrm{RC}} = -C_{\mathrm{RE}} \left[\frac{n_{\mathrm{P}}^2 u_t d_{\mathrm{P}}^2}{\alpha_{\max}^{1/3} (\alpha_{\max}^{1/3} - \alpha^{1/3})} \right] \cdot \left[1 - \exp\left(-C \frac{\alpha_{\max}^{1/3} \alpha^{1/3}}{\alpha_{\max}^{1/3} - \alpha^{1/3}} \right) \right]$$

$$C_{\mathrm{RE}} = 0.004, \quad \alpha_{\max} = 0.75.$$

$$C = 3.0,$$

  - ✓ Coalescence by wake entrainment & phase change

$$R_{\mathrm{WE}} = C_{\mathrm{WE}} C_{\mathrm{D}}^{1/3} n_{\mathrm{P}}^2 d_{\mathrm{P}}^2 |U_{\mathrm{G}} - U_{\mathrm{L}}| \qquad C_{\mathrm{WE}} = 0.002.$$

$$\dot{Q}_{\mathrm{Ph}} = \frac{\pi}{6} d_{\mathrm{Bc}}^3 R_{\mathrm{Pc}}$$

IATE (dynamic flow regime model)

- Two-group IATE
  - Five groups
    - spherical, distorted, cap, Taylor, and irregular-shaped characteristic of the churn-turbulent regime
  - Two groups
    - Spherical or distorted-spherical
    - Larger bubbles: cap bubbles, Taylor bubbles, and irregular-shaped bubbles
  - Boundary between distorted bubbles and cap bubbles

$$V_{\mathrm{B,c}} = \frac{\pi}{6} d_{\mathrm{B,c}}^3 \qquad d_{\mathrm{B,c}} = 4\sqrt{\frac{\sigma}{g(\rho_{\mathrm{L}} - \rho_{\mathrm{G}})}}$$

IATE (dynamic flow regime model)

- Two-group IATE

$$\frac{\partial a''_{\mathrm{I},1}}{\partial t} + \nabla \cdot (a''_{\mathrm{I},1}\vec{U}_{\mathrm{I},1}) = \left[\frac{2}{3} - \chi\left(\frac{d_{\mathrm{sc}}}{d_{\mathrm{Sm},1}}\right)^2\right]\frac{a''_{\mathrm{I},1}}{\alpha_1}\left[\frac{\partial \alpha_1}{\partial t} + \nabla \cdot (\alpha_1 \vec{U}_{\mathrm{G},1}) - \dot{Q}_{\mathrm{ph},1}\right] + \sum_j \phi_{j,1} + \phi_{\mathrm{ph},1}$$

$$\frac{\partial a''_{\mathrm{I},2}}{\partial t} + \nabla \cdot (a''_{\mathrm{I},2}\vec{U}_{\mathrm{I},2}) = \frac{2}{3}\frac{a''_{\mathrm{I},2}}{\alpha_2}\left[\frac{\partial \alpha_2}{\partial t} + \nabla \cdot (\alpha_2 \vec{U}_{\mathrm{G},2}) - \dot{Q}_{\mathrm{ph},2}\right] + \chi\left(\frac{d_{\mathrm{sc}}}{d_{\mathrm{Sm},1}}\right)^2\frac{a''_{\mathrm{I},1}}{\alpha_1}\left[\frac{\partial \alpha_1}{\partial t} + \nabla \cdot (\alpha_1 \vec{U}_{\mathrm{G},1}) - \dot{Q}_{\mathrm{ph},1}\right] + \sum_j \phi_{j,2} + \phi_{\mathrm{ph},2},$$

- Two momentum conservation equations or one momentum equation for mixture of Group 1 and Group2

HW-2

- Flow regime check using Barnea (1985)
  - ✓ Draw the regime transition lines on the $j_g - j_l$ map
  - ✓ Check the change of the lines with the angles
  - ✓ Plot the NEOUR-R data in the $j_g - j_l$ map
  - ✓ Discuss

Chemical Engineering Science, Vol. 40, No. 1, pp. 131–136, 1985.
Printed in Great Britain.

0009–2509/85 $3.00 + 0.00
Pergamon Press Ltd.

GAS–LIQUID FLOW IN INCLINED TUBES: FLOW PATTERN TRANSITIONS FOR UPWARD FLOW

D. BARNEA, O. SHOHAM and Y. TAITEL
Faculty of Engineering, Tel-Aviv University, Ramat-Aviv 69978, Israel

and

A. E. DUKLER
Department of Chemical Engineering, University of Houston, Houston, TX 77004, U.S.A.

(*Received* 28 *October* 1983)

Abstract—Data on flow pattern transitions are presented for upward gas–liquid flow in pipes at inclination angles from 0–90°. Mathematical models previously presented for vertical and horizontal configurations are now extended to cover the full range of pipe inclinations.

INTRODUCTION

Most of the data reported on flow pattern transitions have dealt with either horizontal or vertical tubes with only limited results reported for inclined pipes. Several investigators have considered only one transition for inclined pipes while others have performed experiments only over limited range of inclination angles.

Singh and Griffith (1970) investigated slug flow of air and water at small upward inclination angles and developed simple correlations for pressure drop and holdup. Slug flow in inclined pipes was also treated by Bonnecase *et al.* (1971) who reported data for air–water at angles ranging over ±10° from the horizontal. Beggs and Brill (1973) developed a model for the prediction of pressure drop and holdup in inclined pipes based on the use of holdup correlations for horizontal flow to which a correction factor for the inclination angle is applied. Although data was taken systematically in the full range of ±90° inclination angles, no flow pattern maps were reported. Gould *et al.* (1974) published flow pattern maps for pipes which were horizontal, vertical and inclined at 45°. They concluded that the location of the transition boundaries for the dispersed bubble and annular flow pattern do not vary significantly with inclination.

Experimentally determined flow pattern maps for air–water in a 4.54 cm diameter pipe at angles from vertical upward to vertical downwards were recently reported by Spedding and Nguyen (1980). Empirically located transition boundaries were presented for each inclination angle for which data were reported.

Weisman and Kang (1981) present data for air–water and air–glycerol systems in slightly inclined pipes and for freon–freon vapor systems at inclination angles of 30°, 45° and 90°. Empirical correlations were proposed for the transitions to the annular, dispersed bubble and between the intermittent and bubble flow patterns.

Experimental measurements of flow patterns in slightly inclined pipes were reported by Barnea *et al.* (1980a). The effect of angle on the patterns for downward flow at inclinations ranging from horizontal to vertical was recently investigated by Barnea *et al.* (1982a, b).

The present work reports new data on flow pattern transitions for upward flow of air–water in pipes having inclinations from 0 to 90°. Flow pattern models previously developed for horizontal and slightly inclined pipes (Taitel and Dukler, 1976) and vertical upward flow (Taitel *et al.*, 1980) are extended and modified to provide mechanistic models for estimating the flow pattern transition boundaries over the entire inclination range.

EXPERIMENTAL RESULTS

The experimental apparatus consisted of air and water supply systems and test sections made of two transparent Plexiglass tubes with i.d. of 2.5 and 5.1 cm. respectively. The tubes which were 10 m long were supported on a steel frame capable of varying the angle of inclination continuously in the full range from horizontal to vertical. The flow patterns were determined by visual observation and by oscilloscope display using conductivity probes as suggested by Barnea *et al.* (1980b).

The effect of the inclination angle on the flow pattern transition boundaries was examined by varying the inclination angle in small steps in the range of 0° to 90°. The flow pattern data are presented in Figs 1–16.

Small inclinations from the horizontal have a major effect on the transition from stratified to intermittent or annular pattern. Such inclinations cause intermittent flow to take place over a much wider range of flow rates (Figs 3–16). The stratified-intermittent transition is very sensitive to the angle of inclination. Even for upward slopes of less than 1° the regime of stratified flow shrinks into a small dome shaped region (see Figs 3 and 4). The stratified-smooth pattern is not observed except for angles of less than 0.25°. For values of $U_{Ls} > 0.001$ stratified flow is not observed at all at angles greater than about 20°.

For these small angles the intermittent-annular transition passes to the left of the dome (see Figs 3–8).